SCEC Research Report

Earthquake Petrology: Deformational processes near the Brittle-Plastic Transition

James P. Evans, Department of Geology, Utah State University, Logan, UT 84322-4505
435.797.1267 voice; 435.797.1588 fax james.evans@usu.edu

Proposal Categories: Data gathering and products

Summary

We investigate the deformation mechanisms and slip processes at high temperature conditions, either in the presence of water [hydrothermal conditions] or at frictional heat melt conditions. We target three sites: 1] Aqua Caliente springs, where the rocks adjacent to the Elsinore fault exhibit deformation and hydrothermal alteration, 2] the West Salton Detachment fault, which exhibits pseudotachlylte to semi-brittle slip textures, and 3] the deep Cajon Pass core, where fluid-rock interactions create hydrothermally altered and deformed rocks adjacent to the Cleghorn fault, north of the San Andreas fault.

Agua Caliente Springs lies at the intersection of the NNW-trending Elsinore fault and the 40° NE-dipping inactive West Salton detachment fault. We examine damage zone geometry, fault behavior in crystalline rocks, and the influence of thermal fluids on rock deformation. The Elsinore fault bounds the northwestern flank of the Tierra Blanca Mountains with strike-slip and normal motion; the detachment fault wraps around the northernmost portion of the mountains. Damage along the Elsinore ranges in thickness from a narrow slip plane to > 100 m along the eastern flank of the Tierra Blanca Mountains. Subsidiary faults trend northeast and southeast, and slip orientations vary from normal to strike-slip horizontal motion. Thermal fluids (~30°C) emerge at the intersection of the West Salton detachment and Elsinore faults actively alter the La Posta pluton, already fractured and crushed during fault slip. Fault cores contain thin chlorite ± epidote zones. Cation geothermometry shows the fluids are enriched in Na, Ca, Mg, K, and Si from broken down quartz, plagioclase, and orthoclase. Spring flow increases after seismic events.

The NW-striking West Salton detachment fault (WSDF) is a low-angle normal fault on the western margin of the Salton Trough, California. The fault formed and slipped at a low-angle (<30°) in the brittle crust. We document the presence of 0.1 cm to 2 m-thick, aphanitic, black fault-related rocks with injection structures. Microstructural and electron beam methods established a melt origin for these anomalous fault-rocks. Features include injection structures, quenched margins, spherulites, and a lack of low temperature mineral phases. The documentation of pseudotachylyte along low-angle normal faults is rare and this work helps resolve the debate regarding seismic potential of low-angle normal faults. We continue to establish the structural and geochemical relationships of the pseudotachylyte and other fault rocks in order to incorporate the formation of voluminous pseudotachylyte into models for seismicity of low-angle normal faults.

We performed a systematic structural and geochemical analysis on a suite of cored rocks from the vertical Cajon Pass, California drill hole to characterize the deformation and alteration of fault-related rocks adjacent to the steeply dipping Cleghorn fault which span the brittle to semi-brittle deformational regime at hydrothermal conditions. Fault frequency increases with depth, and fracture densities are greater around fault zones. In the upper 2600 m of the hole, the faults and fractures are narrow with thin coatings of alteration products. Microstructures in these fault zones primarily include shear fractures containing a matrix of laumontite with angular to sub-angular clasts within the matrix and record multiple cycles of deformation and alteration. An indurated, steep-dipping fault zone at 3,402 m depth exhibits a mixture of brittle and semi-brittle deformation and abundant mineralization and alteration of potassium feldspar and epidote. This fault correlates well with the left-lateral steeply dipping Cleghorn fault, and reflects the interaction between hydrothermal and deformation processes at depth and indicates that the faults in the drill hole reflect active deformation and alteration associated with northeast-oriented maximum horizontal stress that may drive the left-lateral oblique motion on the Cleghorn fault. The data also show that damage zones associated with faults are present here, indicating a long-lived presence of the deformed and altered zones of reduced elastic moduli associated with faults, and that semi-brittle distributed shearing may occur at depths as shallow as 3-4 km in the region.

Technical Report

The work we have done includes fieldwork at two sites, and work on core from Cajon Pass core. We perform structural analyses of the rocks, microstructural analyses, and geochemical analyses of fault-related rocks. The Aqua Caliente hydrothermally altered zone lies along the Elsinore fault; the West Salton Detachment fault, and analyses of the deep core from the Cajon Pass scientific drill hole.

Agua Caliente Springs is on the northeastern flank of the Tierra Blanca Mountains in San Diego County, California (Figure 1). Warm springs emerge at the intersection of the active right-lateral Elsinore fault and the inactive West Salton detachment fault damage zones. A left step from the Julian to the Coyote segment of the Elsinore fault at the Tierra Blanca Mountains adds to the complex geometry of the field area (Magistrale and Rockwell, 1996). Faullting and fluids emerging at springs have altered the La Posta tonalite to white-orange kaolinite (Figure 2a). We examined the water chemistry found it necessary to record several attributes of the waters; these attributes are [cations and anions, pH, bicarbonate, temperature, conductivity, water level, and stable isotopes], along with microstructures to examine relationships between local seismicity and spring responses.

Numerous fault zone studies have addressed whether faults behave as conduits, barriers, or both to subsurface fluids (Caine et al., 1996). The Elsinore fault behaves as a conduit for fluid migration along the northeastern side of the Tierra Blanca Mountains. Locations along the Elsinore fault damage zone (Figure 2b). The calcite precipitated out from the fluids into the damaged protolith. Throughout the both fault damage zones grain sizes have been significantly reduced in areas of cataclasite, often breaking down biotite and plagioclase before quartz crystals.

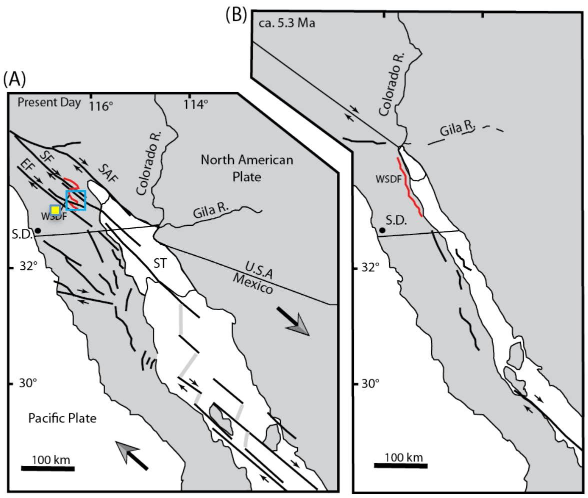

Figure 1: A) Regional tectonic map of the northern Gulf Extensional Province and field area (blue box); B) reconstruction for 5.3 Ma, restoring 350 km of dextral offset on the San Andreas Fault System (modified from Dorsey et al., 2007). EF Elsinore fault, SAF San Andreas fault, SF San Felipe fault, ST Salton Trough, SD San Diego, WSDF West Salton detachment fault. The yellow do indicates the approximate location of the Elsinore fault study areas.

Water chemistry shows that the fluids emerging in the springs are atmospherically sourced based on $\delta^{18}O$ and $\delta^{2}H$ values of -10.1 and -70 respectively. The $\delta^{13}C$ value was -17.5. The spring's pH during November was a slightly basic 9.55. Cations and anions show very low contents of iron and magnesium and high sodium, calcium, potassium, silica, and sulfur values. Spring alkalinity was 180 mg/L. Aqueous geothermometry suggests that a deeper, >150° Tmax,

Figure 1 a. (Top Left) Alteration of the La Posta tonalite protolith to white kaolinite with orange iron streaks; b. (Top Right) Calcite precipitated into a shattered quartz grain within the La Posta tonalite in the Elsinore fault damage zone (2.5x, XPL); c. (Bottom Left) Biotite crystal partially altered to chlorite (10x, PPL); d. (Bottom Right) Laumontite vein in the West Salton detachment fault zone (2.5x, XPL).

source of water interacts with the surface waters, and we suggest there is a fluid channel that has formed at the fault intersection. Spring level data suggest that water levels do change after microseismic swarms 3 km to the NE, but we see not to little pre-swarm temperature, water level, or geochemical anomalies.

The inactive West Salton fault plane lies along the mountain front facing the park is coated in a thin (1/8-1/2") layer of a white, fine-grained powder. Beneath this coating the fault surface is green and there is no alteration on the footwall under this surface suggesting the fault surface acts as a barrier to fluids in that area. The Elsinore fault damage zone is very wide (>100 meters) and is heavily fractured and altered. In one area southeast of the county park there is a fault surface visible along the mountain, and it is identified by a plane coated in calcite. There are numerous subsidiary faults within the Elsinore fault zone and often there are chlorite veins parallel to the slip surface(s).

The West Salton detachment fault lies at the western margin of the Salton Trough (fig. 1) (Schultejann, 1984; Frost and Shafiqullah, 1989; Axen and Fletcher, 1998; Kairouz, 2005; Shirvell et al., 2009; Steely et al., 2009). The Salton Trough lies on the north end of the Gulf Extensional Province, an oblique continental rift that provides insight into rift processes and the transition from initial rifting to formation of oceanic spreading centers (Shirvell et al., 2009; Wong and Gans, 2008; Dorsey, 2010; Umhoefer, 2011). A tectonic model posited by Fletcher et al. (2007) for the formation of the Gulf of California incorporates two stages of rifting and oblique extension. During the first stage, rifting occurred orthogonal to the plate margin and the majority of oblique motion was accommodated by strike-slip faults west of the Baja microplate (Fletcher et al., 2007). Orthogonal rifting occurred from the onset of rifting (12-12.5 Ma) until approximately 6 Ma when the modern transtensional regime formed (Fletcher et al., 2007; Umhoefer, 2011). The West Salton detachment fault is the principal rift-related structure in the Salton Trough (Schultejann, 1984; Frost and Shafiqullah, 1989; Axen and Fletcher, 1998; Shirvell et al., 2009; Steely et al., 2009). The West Salton detachment fault was active from late Miocene to Pleistocene time (Axen and Fletcher, 1998; Cox et al., 2002; King et al., 2002; Matti et al., 2002, 2006; Kairouz, 2005; Steely, 2006; Dorsey et al., 2007; Steely et al., 2009; Shirvell et al., 2009). The detachment fault zone is composed of a damage zone, fault core, and principal slip surface. Fault-related rocks include: fault breccia, cataclasite, ultracataclasite, and an anomalous black fault rock. Thick, laterally extensive, black, aphanitic, fault-related rock occur as detachment-parallel tabular bodies up to 1-m thick in both the

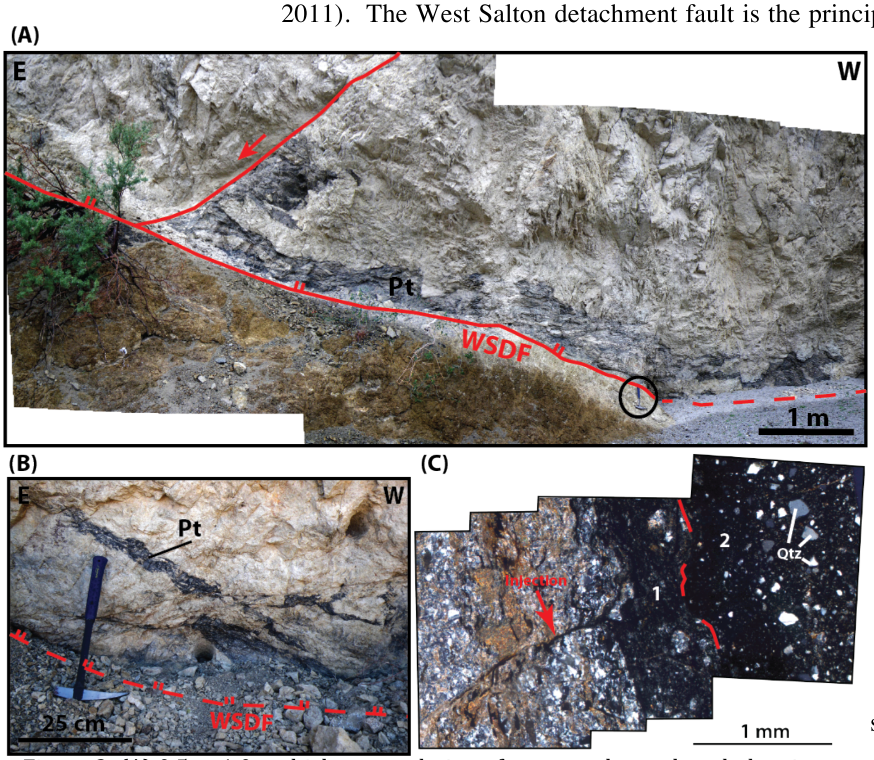

Figure 3: (A) 0.5 to 1.0 m thick accumulation of presumed pseudotachylyte in the immediate hanging wall of the WSDF along the western ling of the Yaqui Ridge anticline, accumulations preserve cm thick layers that have been interpreted to represent multiple injection events. (B) ~4-8 cm thick injection veins in the hanging wall of the WSDF, interpreted to represent pseudotachylyte generated at the principle slip surface. (C) XPL, MP-AB-4-b, photomicrograph of pseudotachylyte vein with small scale injection vein (red arrow) which cross-cuts the protomylonite foliation at a high angle, this example has also been interpreted to represent several injection events based on an observed change in clast abundance and composition (red line), clasts are primarily composed of embayed quartz (Qtz).

hanging and footwall of the main detachment, and planer and curviplanar veins in both the hanging and foot wall of the detachment at high angles and parallel to the main detachment surface (Figure 3). This anomalously thick and laterally extensive black fault rock has been previously identified as probable pseudotachylyte (Schultejahn, 1984; Kairouz et al., 2003; Kairouz, 2005; Steely, 2006; Janecke et al., 2008). These black, aphanitic rocks within the injection structures are typically brittly deformed, and concoidally fractured (Fig. 3B). Petrographic observations of the black fault rock include: injection structures, embayed quartz grains, mm to cm-thick layers of aphanitic material, and faulted quartz and calcite veinlets (Figure 3C). Brittle fractures and faults commonly cross-cut the black, aphanitic fault rock at the microscale (Figure 3C). Scanning electron microscopy observations of the black, aphanitic fault rock include very fine-grained (10-100 μm) subrounded grains, and grains with fibrous overgrowths. These fibrous overgrowths radiate from a central particle and are spherulites, and the embayed quartz grains are consistent with partial melting of minerals in the fault zone. Extremely fine-grained porcelanitic/sintered material with a uniformly very fine grain size dominates the sharp-edged tabular zones. These zones crosscut foliated cataclasites and exhibit multiple episodes of development. Based on the presence of injection structures and melt-related textures (embayed grains, quenched margins, and spherulites) we interpret these aphanitic veins and tabular bodies are pseudotachylyte that formed as a result of friction-induced melt.

The presence of pseudotachylyte in conjunction with geologic evidence that the fault was active at low angles in the brittle-crust suggests that the WSDF was seismically active at low-angles. Though pseudotachylyte has been documented along several low-angle normal faults worldwide, these previously identified melt-related pseudotachylytes have generally been reported from deeper crustal levels. This finding has significant implications for the ongoing debate regarding the seismic potential of low-angle normal faults in the brittle crust (e.g. Wernicke, 1995; Axen, 2004; Abers, 2009). The preliminary results of this study have been presented (Janecke et al., 2008; Prante et al., 2011). Future work includes XRD and XRF analyses focused on understanding mineralogic and chemical changes across the fault zone. This work is focused on understanding fluid-fault interaction in an effort the better understand the nature of paleoseismicity on the West Salton detachment fault. These results also have significant implications for the low-angle normal fault paradox. This study provides an opportunity to investigate tectonic pseudotachylyte from an environment typically though to be unfavorable to frictional melt generation (Sibson and Toy, 2006).

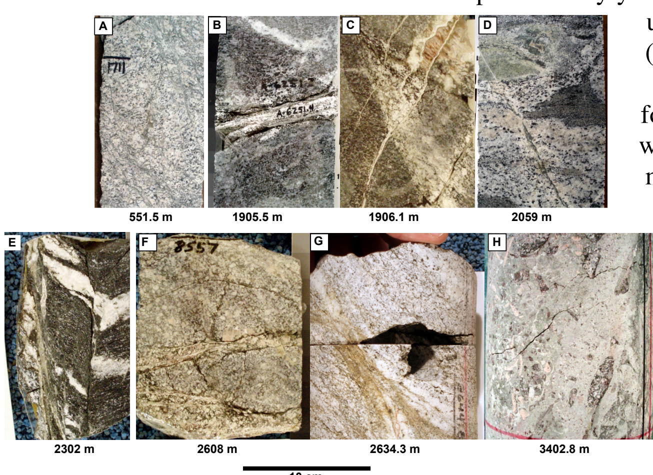

Figure 4. Views of key mesoscopic structures in the core. A. Thin chloritic shear zones that dip steeply. B. Shallowly dipping zeolite-chlorite shear zone C. Narrow steep dipping laumonitite veins D. Narrow chlorite shear zone. E. Nearly vertical chlorite + zeolite+ epidote decorated shear zones that cut the white and green banding in the gneiss. F. Laumontite – chlorite shear zones at a low- angle to the core axis from 2608 m md. G. Moderately dipping semi-brittle shear zone H. Indurated shear zone at 3402.8 m md.

The work on the Cajon Pass drill core focused on analyses of core materials and the wireline log data from the project to infer mechanical properties and deformation mechanisms at depth. The most notable core samples come from 3402 m measured depth [Figure 4h] which samples a semibrittle shear zone that is comprised of fractures, veins, and laumontite. Grain-size reduction, microfractures, and mineral alteration, to varying degrees are seen throughout the majority of samples. Some of the microstructures from the Cajon Pass do show evidence of repeated stress/strain cycling, based on evidence of undeformed laumontite crystals surrounded by a matrix of fine-grained and fractured laumontite.

Wireline log data (Figure 5) indicate a complex signature between the faulted rocks and their log signatures. Of the 23 faults between 1900 and 3415 m md, faults between 2260 and 2536 m md, and the faults the between 3136 and 3172 m md, exhibit what we might term "typical" log response, in which the sonic velocities are reduced relative to the host rock, and porosities increase. In only three zones (2140, 2317, and 2439 m md) does resistivity decrease, and the gamma ray log exhibits little change. The larger fault zones were identified by previous workers (Barton and Zoback, 1992; Blenkinsop and Sibson, 1992; Vernik and Zoback, 1992) are marked by decreases in V_s and V_p values, and increased fracture density (Figure 5). The largest fault zones as determined by wireline log data are at 2439-2526 m and 3180-3204 m depths have the largest fracture apertures. Increases in the drilling rate of penetration (ROP) also coincide with the presence of faults and fracture zones. The lower 300 m of the borehole exhibits an increase in the mean values and variability of resistivity and gamma ray signatures, suggesting a change in either the protolith character and/or influence from the mineralized faults.

We suggest that the several of the fault zones identified in the core and in the synthesis of the wireline data correlate with faults mapped on the surface. Specifically, The fault zones at 3400 m correlates up dip at approximately 75° and projects upward to the surface trace of the nearby left lateral strike-slip Cleghorn fault. The surface trace of the Cleghorn fault has a dip that ranges from 70° to vertical (Meisling, 1984) ~1.5 km away from the borehole.

Outreach activities - Our primary outreach activity involved a 2010 undergraduate research project funded by SCEC, the Eastern Los Angeles Community College, and USU research funds. Four undergraduates from USU, Wesylean, ELAC, and UBC worked on a project that is an outgrowth of the Aqua Caliente project, in which the students examined the water chemistry, temperature, and earthquake frequency of the Davis-Schrimpf hot springs at the southeastern edge of the Salton Sea. This work helped determine maximum water tempeartures of > 150° C, and a weak correlation between water temperature fluctuations and the seismicity with a 5 km radius. Preliminary data were presented in Shervais et al., 2011, and the educational component was presented in Ponce-Zepeda et al., 2011a,b.

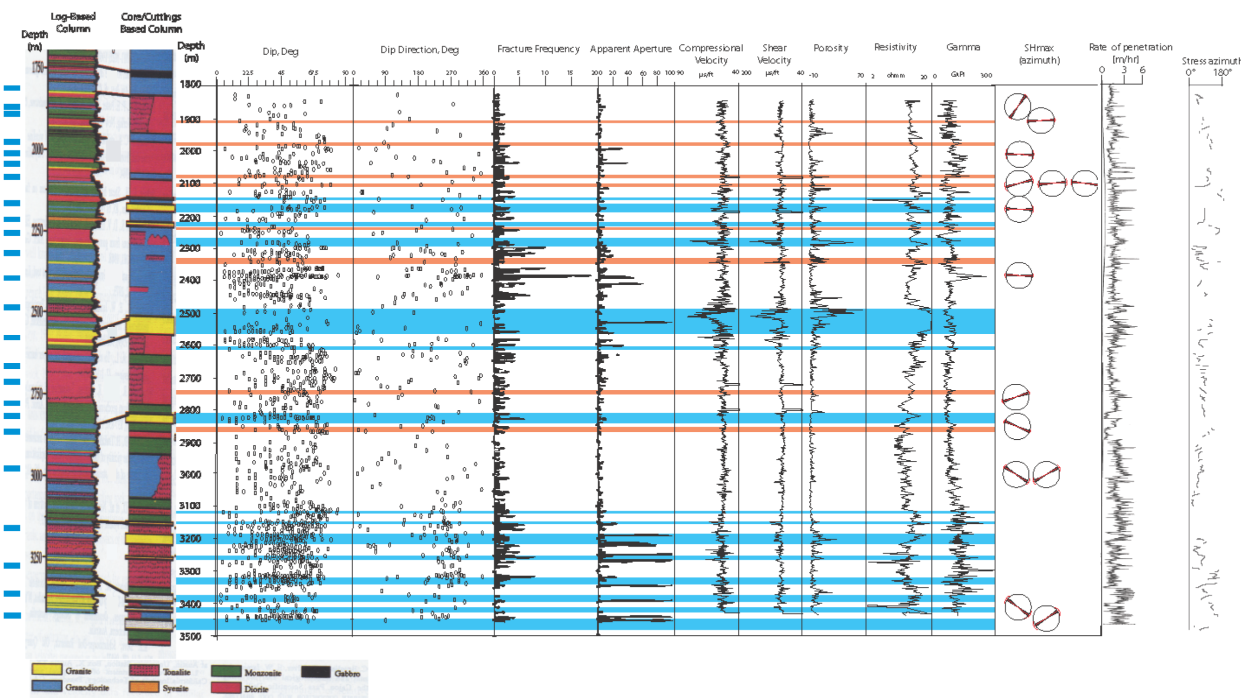

Figure 5. Lithologic column of the crystalline core and Cajon Pass borehole from depths 1800 m to 3500 m with wireline log data, structural data from this work and that of previous workers, stress orientation data, and rate of penetration data. Revised lithologic column, dip and dip direction, fracture density, apparent fracture aperture, V_p, V_s, porosity, resistivity, gamma logs are from Barton and Zoback (1992). The $\sigma_H$max data are from Zoback and Healy (1992), Shamir (1990), Shamir and Zoback (1992) and Day-Lewis and Zoback (2010). The rate of penetration data are digitized from Shamir (1990). North is marked at the top of the column and the red lines around the circles represent associated error with each measurement. Orange lines mark locations of newly identified faults from this study. Blue lines represent previously identified faults.

References

Abers, G., 2009, Slip on shallow-dipping normal faults: Geology, v. 37, p. 767-768.

Anderson, R. N., Dove, R. Silver, L. James, E. and Chappell, B. 1988b, Elemental and Mineralogical Analyses Using Geochemical Logs from the Cajon Pass Scientific Drillhole, California, and their Preliminary Comparison with Core Analyses: Geophysical Research Letters, v. 15, p. 969–973.

Anderson, R.N., Broglia, C., Pezard, P.A., and Williams, C.F. 1988a, Lithostratigraphy Determined from Discriminate Analysis of Geochemical Well Logs from the Cajon Pass Scientific Drillhole, California: Geophysical Research Letters, v. 15, p. 957-960.

Axen, G. J., and Fletcher, J., 1998, Late Miocene-Pleistocene Extensional Faulting, Northern Gulf of California, Mexico and Salton Trough, California: International Geology Review, v. 40, p. 217-244.

Axen, G.J., 2004, Mechanics of low-angle normal faults, *in* Karner, G.D., et al., eds., Rheology and Deformation of the Lithosphere at Continental Margins: New York, ColumbiaUniversity Press, p. 46–91.

Barton, C.A., and Zoback, M.D., 1992, Self-similar distribution and properties of macroscopic fractures at depth in crystalline rock in the Cajon Pass scientific drill hole: Journal of Geophysical Research, v. 97, p. 5181-5200.

Blakeslee, S., Malin, P.,Alvarez, M., 1989, Fault-Zone attenuation of high-frequency seismic waves, Geophysical Research Letters, v. 16, p. 1321-1324.

Blenkinsop, T.G., 1990, Correlation of paleotectonic fracture and microfracture orientations in cores with seismic anisotrophy at Cajon Pass drill hole, southern California: Journal of Geophysical Research, v. 95, p. 11143-11150.

Blenkinsop, T.G., and Sibson, R.H., 1992, Aseismic fracturing and cataclasis involving reaction softening within core material from the Cajon Pass Drill Hole: J. Geophysical Res, v. 97, p. 5135-5143.

Caine, J.S., Evans, J.P., and Forster, C.B., 1996, Fault zone architecture and permeability structure: Geology, v. 24, p. 1025-1028.

Chester, F.M., and Logan, J.M., 1987, Composite Planar Fabric of Gouge from the Punchbowl Fault, California: Journal of Structural Geology, v. 9, p. 621-634.

Chester, F.M., Evans, J.P., and Biegel, R.L., 1993, Internal structure and weakening mechanisms of the San Andreas Fault: Journal of Geophysical Research, v. 98, p.771-786.

Cochran, E. S., Li, Y.-G., Shearer, P. M., Barbot, S., Fialko, Y., and Vidale, J. E., 2009, Seismic and geodetic evidence for extensive, long-lived fault damage zones, Geology, v. 37, p. 315-318, doi: 10.1130/G25306A.1.

Cox, B. F., Matti, J.C., King, T., and Morton, D.M., 2002, Neogene strata of southern Santa Rosa Mountains, California, and their significance for tectonic evolution of western Salton Trough: Geological Society of America Abstract with Programs, v. 34, p. 124.

Day-Lewis, A. D. F., Zoback, M, and Hickman, S., 2010, Scale-invariant stress orientations and seismicity rates near the San Andreas Fault, Geophysical Research Letters, v. 37, L 24304, doi: 10.1029/2010GL045025.

Dorsey, R. J., Fluette, A., McDougall. K. A., Housen, B. A., Janecke, S. U., Axen, G. A., and Shirvell, C. R., 2007, Chronology of Miocene-Pliocene deposits at Split Mountain Gorge, southern California: A record of regional tectonics and Colorado River evolution: Geology, v. 35, p. 57–60.

Dorsey, R.J., 2010, Sedimentation and crustal recycling along an active oblique-rift: Salton Trough and northern Gulf of California: Geology, v. 38, p. 443-446.

Fletcher, J. M., Grove, M., Kimbrough, D., Lovera, O., and Gehrels, G.E., 2007, Ridge-trench interactions and the Neogene tectonic evolution of the Magdalena shelf and southern Gulf of California: Insights from detrital zircon U-Pb ages from the Magdalena fan and adjacent areas: Geological Society of America Bulletin, v. 119, p. 1313–1336.

Fuis, G.S., Scheirer, D.S., Langenhein, V.E., Kohler, M.D., 2008, The San Andreas Fault in southern California has a “propeller” shape-implications for tectonics and seismic hazard: Geological Society of America Abstracts with programs, v. 40, no. 6, p.326.

Hardebeck, J.L., and Michael, A. J., 2004, Stress orientations at intermediate angles to the San Andreas fault, California: Journal of Geophysical Research, v. 109, p. 11303.

Imber, J, Holdsworth, R.E, Butler, C.A & Strachan, R.A 2001. A reappraisal of the Sibson-Scholz fault zone model: The nature of the frictional to viscous (‘brittle-ductile’) transition along a long-lived crustal-scale fault, Outer Hebrides, Scotland. Tectonics **v.** 20, p. 601-624.

Jacobs, J. R., and Evans, J. P, and Kolesar, P. T.,2006, Chemical alteration in fault zones as sinks for "missing" earthquake energy, in: R. Abercrombie, H. Kanamori, and G. di Toro, eds., Earthquakes: Radiated Energy and the Physics of Faulting, American Geophysical Union Geophysical Monograph 170, p. 181-192.

Janecke, S.U., Steely, A.N., Evans, J.P., 2008, Seismic Slip on an Oblique Detachment Fault at Low Angles: Eos Trans. AGU, v. 89, Fall Meeting Suppl., Abstract T53F-06.

Kairouz, M., 2005, Geology of the Whale Peak region of the Vallecito Mountains: Emphasis on the kinematics and timing of the west Salton detachment fault, southern California [M.S. thesis], University of California, Los Angeles, p. 166.

Kairouz, M., Axen, G.J., Grove, M., Lovera, O., and Stockli, D.F., 2003, Late Cenozoic 40Ar/39Ar ages of fault rocks formed along the West Salton detachment system, southern California, Geological Society of America Abstracts with Programs, v. 35, p. 629.

Kharaka, Y.K., Ambats, G., Evans, W.C., and White, A.F., 1988, Geochemistry of water at Cajon Pass, California: preliminary results: Geophysical Research Letters, v. 15, p. 1037-1040.

Lachenbruch, A.H., and Sass, J.H., 1988, The stress heat-flow paradox and thermal results from Cajon Pass: Geophysical Research Letters, v. 15, p. 981-984.

Leary, P. C., Henyey, T. L., and Li, Y.-G., 1988, Fracture related reflectors in basement roc from vertical seismic profiling at Cajon Pass, Geophysical Research Letters, v. 15, p. 1057-1060.

Leary, P.C., 1991, Deep borehole evidence for fractal distribution of fractures in crystalline rock, Geophysical Journal International, v. 107, p. 615-627.

Magistrale, H., and Rockwell, T., 1996, The Central and Southern Elsinore Fault Zone, Southern California: Bulletin of the Seismological Society of America, v. 86, p. 1793-1803.

Matti, J. C., Cox, B.F., Morton, D.M., Sharp, R.V., and King, T., 2002, Fault-bounded Neogene sedimentary deposits in the Santa Rosa Mountains, southern California: Crustal stretching or transpressional uplift? Geological Society of America Abstracts with Programs, v. 34, p. 124.

Matti, J. C., Morton, D.M., Cox, B.F., Landis, G.P., Langenheim, V.E., Premo, W.R., Kistler, R., and Budahn J.R., 2006, Fault-bounded late Neogene sedimentary deposits in the Santa Rosa Mountains, southern CA: Constraints on the evolution of the San Jacinto fault, Eos Trans. AGU, v. 87(52), Fall Meet. Suppl., Abstract T21B-0407.

Meisling, K.E., and Weldon, R.J., 1989, Late Cenozoic tectonics of the northwestern San Bernardino Mountains, southern California: Geological Society of America Bulletin, v.101, p. 106-128.

Mitchell, T. M., and Faulkner, D. R, 2009, The nature and origin of off-fault damage surrounding strike-slip faults with a wide range of displacements: A field study from the Atacama fault, northern Chile, Journal of Structural Geology, v. 31, p. 802-816.

Morton, D.M., and Miller, F.K., 2006, Geologic map of the San Bernardino and Santa Ana 30' x 60' quadrangles, California: Geological Survey Open-File report 2006-1217, scale 1:100000, 4 sheets, 200 p. text.

Pechnig, R., Delius, H., and Bartetzko, A., 2005, Effects of composition variations on log responses of igneous and metamorphic rocks, II: acid and intermediate rocks, in: Harvey, P. K., Brewer, T. S., Pezard, P. A., and Petrov, V. A., eds., Petrophysical Properties of crystalline rocks, Geological Society of London Special Publication 240, p. 179-300.

Pezard, P.A., Anderson R.N., Howard, J.J., Luthi, S.M., 1988a, Fracture distribution and basement structure from measurements of electrical resistivity in the basement of the Cajon Pass scientific drillhole, California: Journal of Geophysical Research Letters, v. 15, p. 1021-1204.

Ponze-Zepeda, M., 2011a, MESA – Not just a seat at the table: A Chicano Geology's student experience with investigative field research, Geol. Soc. Abstracts Meeting 70-11..

Ponze-Zepeda, M., 2011b, MESA – Not just a seat at the table: A Chicano Geology's student experience with investigative field research, AGU Abstracts, Fall Meeting ED11E-03.

Prante, M.R., Evans, J.P., Janecke, S.U., 2011, Paleoseismicity along a low-angle normal fault: Evidence from the Salton Trough, CA, USA: Abstract T41C-07 presented at 2011 Fall Meeting, AGU, San Francisco, Calif., 5-9 Dec.

Sass, J.H., Lachenbruch, A.H., Moses Jr., T.H., and Morgan, P., 1992, Heat flow from a scientific research well at Cajon Pass, California: Journal of Geophysical Research, v. 97, p. 5017-5029.

Saucier, F., Humphreys, E., and Weldon, R. J. II, 1992, Stress near geometrically complex strike-slip faults: application to the San Andreas Fault at Cajon Pass, southern California, Journal of Geophysical Research, v. 97, p 5081-5094.

Scholz, C.H., 2000, Evidence for a strong San Andreas fault: Geology, v. 28, p. 163-166.
Scholz, C.H., 2006, The strength of the San Andreas fault; a critical analysis: in: R. Abercrombie, H. Kanamori, and G. di Toro, eds., Earthquakes: Radiated Energy and the Physics of Faulting, American Geophysical Union Geophysical Monograph, v. 170, p. 301-311.
Scholz, C.H., and Saucier, F.J., 1993, What do the Cajon Pass stress measurements say about stress on the San Andreas fault ?: Journal of Geophysical Research, v. 98, p. 17867-17869.
Schultejann, P.A., 1984, The Yaqui Ridge antiform and detachment fault: Mid-Cenozoic extensional terrane west of the San Andreas fault: Tectonics, v. 3, no. 6, p. 677–691.
Shamir, G., and Zoback, M.D., 1992, Stress orientation profile to 3.5 km depth near the San Andreas fault at Cajon Pass, California: Journal of Geophysical Research, v. 97, p.5059-5080.
Shervais, K., Young, B., Ponce-Zepeda, M., and Rosove, S., 2011, Integrated Field Analyses of Thermal Springs, AGU Abstracts, Fall Meeting, H51C-1224.
Shirvell, C.R., Stockli, D.F., Axen, G.J., Grove, M., 2009, Miocene-Pliocene exhumation along the west Salton detachment fault, southern California, from (U-Th)/He thermochronometry of apatite and zircon: Tectonics, v. 28, TC2006.
Sibson, R.H., and Toy, V.G., 2006, The Habitat of Fault-Generated Pseudotachylyte: Presence vs. Absence of Friction-Melt, in, AGU Geophysical Monograph Series, v. 170, p. 153-166.
Silver, L.T., and James, E.W., 1988, Geologic setting and lithologic column of the Cajon Pass Deep Drillhole: Geophysical Research Letters, v. 15, p. 941-944.
Silver, L.T., James, E.W., and Chappell, B.W., 1988, Petrological and geochemical investigations at the Cajon Pass deep drillhole: Geophysical Research Letters, v. 15, p. 961-964.
Spotila, J.A., House, M.A., Blythe, A.E., Niemi, N.A., and Bank, G.C., 2002, Controls on the erosion and geomorphic evolution of the San Bernardino and San Gabriel Mountains, southern California, in Barth, A., ed., Contribution to crustal evolution of the southwestern United States: Boulder, Colorado, Geological Society of America Special Paper 365, p. 205-230.
Steely, A.N., 2006, The evolution from late Miocene west Salton detachment faulting to cross-cutting Pleistocene oblique strike-slip faults in the SW Salton Trough, southern California [M.S. thesis]: Utah State University, 364 p.
Steely, A.N., Janecke, S.U., Dorsey, R.J., Axen, G.J., 2009, Early Pleistocene initiation of the San Felipe fault zone, SW Salton Trough, during reorganization of the San Andreas fault system: Geological Society of America Bulletin, v. 121, p. 663-687.
Townend, J., and Zoback, M. D., 2004, Regional tectonic stress near the San Andreas fault inc central and southern California, Geophysical Research Letters, v. 31, doi:10.1029/2003GL018918.
Umhoefer, P.J., 2011, Why did the Southern Gulf of California rupture so rapidly? Oblique divergence across hot, weak lithosphere along a tectonically active margin: GSA Today, v. 21, p. 4-10.
Vernik, L., and Zoback, M.D., 1992, Estimation of maximum horizontal principal stress magnitude from stress-induced well bore breakouts in the Cajon Pass scientific research borehole: Journal of Geophysical Research, v. 97, p. 5107-5119.
Vincent, M.W., and Ehlig, P.L., 1988, Laumontite mineralization in rocks exposed north of the San Andreas fault at Cajon Pass, southern California: Geophysical Research Letters, v. 15 p. 977-980.
Wallace, R.E., 1990, General Features: The San Andreas Fault System, California, USGS Professional Paper 1515, p. 3-12.
Wernicke, B., 1995, Low-angle normal faults and seismicity: A review: Journal of Geophysical Research, v. 100, p. 20159–20174.
Wibberley, C. A. J., G. Yielding, and G. Di Toro, 2008, Recent advances in the understanding of fault zone structure, *in* C.A.J. Wibberley, W. Kurz, J. Imber, R.E. Holdsworth, and C. Coletinni, eds., The internal structure of fault zones: Implications for mechanical and fluid-flow properties: Geological Society of London Special Publication 299, p. 5-33.
Zoback, M.D., and Healy, J.H, 1992, In situ stress measurements to 3.5 km depth in the Cajon Pass scientific research borehole: implications for the mechanics of crustal faulting: Journal of Geophysical Research, v. 97, p. 5039-5058.